

# Bouncing localized structures in a Liquid-Crystal-Light-Valve experiment

M.G. Clerc†, A. Petrossian and S. Residori

*Institut Non-Linéaire de Nice, 1361 Route des Lucioles, 06560 Valbonne, France*

† *Departamento de Física, Facultad de Ciencias Físicas y Matemáticas,  
Universidad de Chile, Casilla 487-3, Santiago, Chile.*

(Dated: February 9, 2018)

Experimental evidence of bouncing localized structures in a nonlinear optical system is reported. Oscillations in the position of the localized states are described by a consistent amplitude equation, which we call the Lifshitz normal form equation, in analogy with phase transitions. Localized structures are shown to arise close to the Lifshitz point, where non-variational terms drive the dynamics into complex and oscillatory behaviors.

Pacs: 05.45.-a, 42.65.Sf, 47.54.+r

During the last years localized structures have been observed in different fields, such as domains in magnetic materials [1], chiral bubbles in liquid crystals [2], current filaments in gas discharge experiments [3], spots in chemical reactions [4], pulses [5], kinks [6] and localized 2D states [7] in fluid surface waves, oscillons in granular media [8], isolated states in thermal convection [9, 10], solitary waves in nonlinear optics [11, 12, 13] and cavity solitons in lasers [14]. Localized states are patterns which extend only over a small portion of a spatially extended and homogeneous system [15]. Different mechanisms leading to stable localization have been proposed [16]. Among these, two main classes of localized structures have to be distinguished, namely those localized structures arising as solutions of a quintic Swift-Hohenberg like equation [16] and those that are stabilized by non-variational terms in the subcritical Ginzburg-Landau equation [17]. The main difference between the two cases is that the first-type localized structures have a characteristic size which is fixed by the pinning mechanism over the underlying pattern or by spatial damped oscillations between homogenous states [16, 18], whereas the second-type ones have no intrinsic spatial length, their size being selected by non-variational effects and going to infinity when dissipation goes to zero. In both cases, non-variational effects may lead to dynamical behaviors of localized structures [19]. Variational models based on a generalized Swift-Hohenberg equation have been proposed to describe the appearance of localized structures in nonlinear optics [20]. However, a generalization including non-variational terms is generically expected to apply even in optics, as happens, for instance, in semiconductor laser instabilities [21], giving rise to dynamical behaviors of localized structures, such as propagation and oscillations of their positions [22].

We report here an experimental evidence of localized structures dynamics in a Liquid-Crystal-Light-Valve (LCLV) with optical feedback. It is already known that, in the simultaneous presence of bistability and pattern forming diffractive feedback, the LCLV system shows localized structures [12, 23, 24, 25]. Recently, rotation of localized structures along concentric rings have been re-

ported in the case of a rotation angle introduced in the feedback loop [26]. Here, we fix a zero rotation angle and we show a new dynamical behavior, the bouncing of two adjacent localized structures, that is not related to imposed boundary conditions but is instead a direct consequence of the non-variational character of the system under study. Theoretically, we show that the LCLV system has several branches of bistability connecting an homogeneous state to a patterned one and we derive an amplitude equation accounting for the appearance of localized structures. This is a one-dimensional model, that we call the Lifshitz normal form equation [22], characterizing the dynamics of localized structures close to each point of nascent bistability.

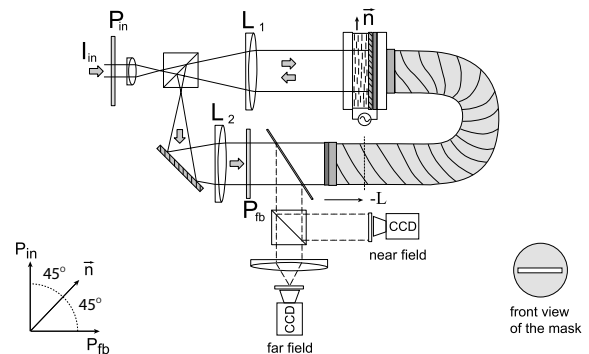


FIG. 1: Experimental setup:  $\vec{n}$  liquid crystal nematic director;  $P_{in}$  and  $P_{fb}$  input and feedback polarizers;  $L_1$  and  $L_2$  confocal 25 cm focal length lenses.  $-L$  is the free propagation length, negative with respect to the plane on which a 1:1 image of the front side of the LCLV is formed.

*Description of the experiment.* The experimental setup is shown in Fig.1. The LCLV is composed of a nematic liquid crystal film sandwiched in between a glass and a photoconductive plate over which a dielectric mirror is deposited. The liquid crystal film is planar aligned (nematic director  $\vec{n}$  parallel to the walls), with a thickness  $d = 15 \mu\text{m}$ . The liquid crystal filling our LCLV is the nematic LC-654, produced by NIOPIK (Moscow) [27]. It is a mixture of cyano-biphenyls, with a positive dielectric anisotropy  $\Delta\epsilon = \epsilon_{\parallel} - \epsilon_{\perp} = +10.7$  and large optical birefringence,  $\Delta n = n_{\parallel} - n_{\perp} = 0.2$ , where  $\epsilon_{\parallel}$  and  $\epsilon_{\perp}$  are the

dielectric permittivities  $\parallel$  and  $\perp$  to  $\vec{n}$ , respectively, and  $n_{\parallel}$  and  $n_{\perp}$  are the extraordinary ( $\parallel$  to  $\vec{n}$ ) and ordinary ( $\perp$  to  $\vec{n}$ ) refractive index, respectively. Transparent electrodes over the glass plates permit the application of an electrical voltage across the liquid crystal layer. The photoconductor behaves like a variable resistance, which decreases for increasing illumination. The feedback is obtained by sending back onto the photoconductor the light which has passed through the liquid-crystal layer and has been reflected by the dielectric mirror. This light beam experiences a phase shift which depends on the liquid crystal reorientation and, on its turn, modulates the effective voltage that locally applies to the liquid crystals.

The feedback loop is closed by an optical fiber bundle and is designed in such a way that diffraction and polarization interference are simultaneously present [12]. The optical free propagation length is fixed to  $L = -10$  cm. At the linear stage for the pattern formation, a negative propagation distance selects the first unstable branch of the marginal stability curve, as for a focusing medium. The angles of the polarizers are at  $45^\circ$  with respect to the liquid crystal director  $\vec{n}$ . The free end of the fiber bundle is mounted on a precision rotation and translation stage, to avoid rotation or translation in the feedback loop.

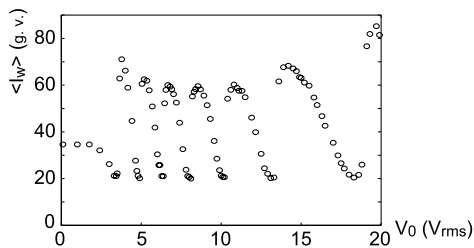


FIG. 2: Spatially averaged feedback intensity  $\langle I_w \rangle$  (units are the gray values, g.v., on the CCD camera) as a function of  $V_0$ ; input intensity  $I_{in} = 0.75$  mW/cm<sup>2</sup>.

For this parameter setting, as  $V_0$  increases there is a series of successive branches of bistability between a periodic pattern and a homogeneous solution. In Fig.2 we report the spatially averaged feedback intensity  $\langle I_w \rangle$  measured for a fixed value of the input intensity,  $I_{in} = 0.75$  mW/cm<sup>2</sup>, and for varying  $V_0$ , by integrating the images on the near-field CCD camera (see Fig.1). The abrupt changes of  $\langle I_w \rangle$  correspond to the appearance of localized structures and thus roughly indicate the locations of the nascent bistability points. The peak value intensity of the localized structures is approximately twice the average value  $\langle I_w \rangle$ . In the LCLV system, the bistability between homogenous states results from the subcritical character of the Fréedericksz transition, when the local electric field, which applies to the liquid crystals, depends on the liquid crystal reorientation angle [28, 29]. Here, we limit our study to the bistable branch located around  $V_0 = 13.2$  V<sub>rms</sub> (frequency 5 KHz), however similar observations can be obtained close to any other of the

nascent bistability points.

We have carried out one-dimensional experiments, in order to avoid the influence of any optical misalignment (such as small drifts) on the dynamics of localized states. A rectangular mask is introduced in the optical feedback loop, just in contact to the entrance side of the fiber bundle. The width of the aperture is  $D = 0.50$  mm whereas its length is  $l = 20$  mm. The size of each localized structure is  $\Lambda \simeq 350$   $\mu$ m, so that the transverse aspect ratio  $D/\Lambda \simeq 1$  is small enough for the system to be considered as one-dimensional and the longitudinal aspect ratio  $l/\Lambda \simeq 60$  is large enough for the system to be considered as a spatially extended one.

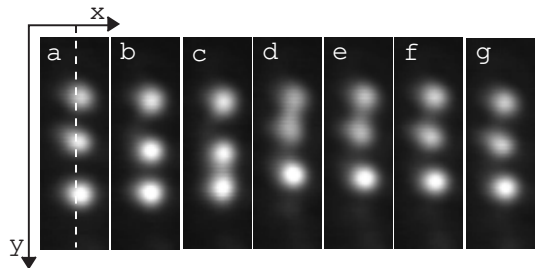


FIG. 3: Snapshots showing bouncing localized structures; a)  $t = 0.0$ , b) 1.0, c) 1.3, d) 1.7, e) 2.1, f) 2.4, g) 2.8 sec.

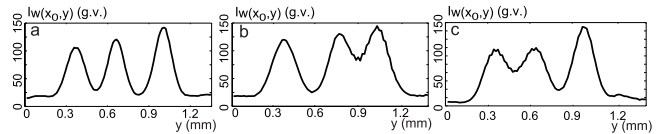


FIG. 4: Localized structures profile,  $I_w(x_0, y)$ ;  $x_0$  is the location of the dashed line in Fig.3; a)  $t = 0.0$  b) 1.3, c) 1.7 sec.

Instantaneous snapshots of bouncing localized structures, together with their spatial profiles, are shown in Fig.3, for  $V_0 = 13.2$  V<sub>rms</sub> and  $I_{in} = 0.95$  mW/cm<sup>2</sup>. The corresponding spatio-temporal plot is displayed in Fig.5b, showing the periodic oscillations for the positions of the structures. In the same figure, Fig.5a, it is shown the spatio-temporal plot corresponding to stationary localized structures, as observed for a slightly decreased input intensity,  $I_{in} = 0.90$  mW/cm<sup>2</sup>, and for the same value of  $V_0$ . Fig.5c displays the spatio-temporal diagram corresponding to aperiodic oscillations in the structure positions, as observed for  $V_0 = 13.3$  V<sub>rms</sub> and  $I_{in} = 0.90$  mW/cm<sup>2</sup>. The dynamical behavior of localized structures is very sensitive to parameter changes and, even though their appearance is clearly located around each point of nascent bistability, their stability range is smaller than the width of the bistable region. When losing stability, localized structures either form clusters or annihilate, depending if they are driven on the pinning or depinning side of the bistable region [18]. However, a

careful experimental characterization of the pinning front is a work still in progress.

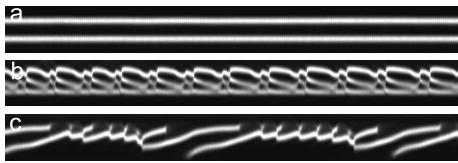


FIG. 5: Space(vertical)-time (horizontal) diagrams showing a) two stationary localized structures, b) periodic and c) aperiodic oscillations of the structure positions. The total elapsed time is 94 s.

*Theoretical description.* The light intensity  $I_w$  reaching the photoconductor is given by [12],  $I_w = \frac{I_{in}}{2} |e^{-i\frac{\Gamma}{2k}\partial_{xx}}(1 + e^{-i\beta\cos^2\theta})|^2$ , where  $x$  is the transverse direction of the liquid crystal layer,  $\beta\cos^2\theta$  is the overall phase shift experienced by the light travelling forth and back through the liquid crystal layer;  $\beta = 2kd\Delta n$ , where  $k = 2\pi/\lambda$  is the optical wave number ( $\lambda = 633$  nm).

As long as  $I_{in}$  is sufficiently small, that is, of the order of a few  $mW/cm^2$ , the effective electric field,  $E_{eff}$ , applied to the liquid crystal layer can be expressed as  $E_{eff} = \Gamma V_0/d + \alpha I_w$ , where  $V_0$  is the voltage applied to the LCLV,  $0 < \Gamma < 1$  is a transfer factor that depends on the electrical impedances of the photoconductor, dielectric mirror and liquid crystals and  $\alpha$  is a phenomenological dimensional parameter that describes the linear response of the photoconductor [29].

Let us call  $\theta(x, t)$  the average director tilt.  $\theta = 0$  is the initial planar alignment whereas  $\theta = \pi/2$  is the homeotropic alignment corresponding to saturation of the molecular reorientation. The dynamics of  $\theta$  is described by a local relaxation equation of the form

$$\tau\partial_t\theta = l^2\partial_{xx}\theta - \theta + \frac{\pi}{2} \left( 1 - \sqrt{\frac{\Gamma V_{FT}}{\Gamma V_0 + \alpha d I_w(\theta, \partial_x)}} \right) \quad (1)$$

with  $V_{eff} = E_{eff}d = \Gamma V_0 + \alpha d I_w(\theta, \partial_x) > V_{FT}$  the effective voltage applied to the liquid crystals,  $V_{FT}$  the threshold for the Fréedericksz transition and  $l$  the electric coherence length. The above model have been deduced by fitting the experimental data for the open loop response of the LCLV [29] and it is slightly different with respect to the one proposed in Ref. [12]. It is important to note that a rigorous derivation of the response function of the LCLV would require a modal expansion along the longitudinal direction of the liquid crystal layer.

The homogeneous equilibrium solutions are  $\theta_0 = 0$  when  $V_{eff} \leq V_{FT}$  and  $\theta_0 = \pi/2 \left( 1 - \sqrt{V_{FT}/V_{eff}} \right)$  when  $V_{eff} > V_{FT}$ . Above Fréedericksz transition and by neglecting the spatial terms we can find a closed expression for the homogeneous equilibrium solutions:  $\theta_0 = \pi/2 \left( 1 - \sqrt{V_{FT}/(\Gamma V_0 + \alpha I_{in}[1 + \cos(\beta \cos^2 \theta_0)])} \right)$ .

The value of  $V_{FT}$  is set to  $3.2 V_{rms}$ , as measured for the LCLV [28, 29], and the graph of  $\theta_0(V_0, I_{in})$  is plotted in Fig.6. In agreement with the bistability branches observed experimentally, several points of nascent bistability can be distinguished, corresponding to the critical points where  $\theta_0(V_0, I_{in})$  becomes a multi-valued function.

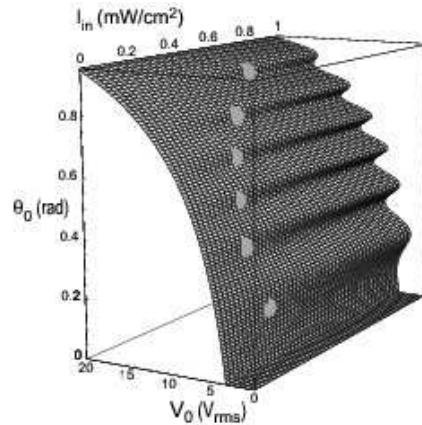


FIG. 6: The multi-valued function  $\theta_0(V_0, I_{in})$ . Shaded areas show the location of the nascent bistability points.

Close to each point of nascent bistability, and neglecting spatial derivatives, we can develop  $\theta = \theta_0 + u + \dots$  and derive a normal form equation describing an imperfect pitchfork bifurcation [15],  $\partial_t u = \eta + \mu u - u^3 + h.o.t.$ , where  $\mu$  is the bifurcation parameter and  $\eta$  accounts for the asymmetry between the two homogeneous states. Higher order terms are ruled out by the scaling analysis, since  $u \sim \mu^{1/2}$ ,  $\eta \sim \mu^{3/2}$  and  $\partial_t \sim \mu$ ,  $\mu \ll 1$ . If we now consider the spatial effects, due to the elasticity of the liquid crystal and to the light diffraction, the system exhibits a spatial instability as a function of the diffraction length and, since the spatial dependence of  $I_w$  is nonlocal, the dynamics is a non-variational one.

The confluence of bistability and spatial bifurcation give rise to a critical point of codimension three, that we call the Lifshitz point, in analogy with the triple point introduced for phase transitions in helicoidal ferromagnetic states [30]. Close to this point, we derive an amplitude equation, that we call the Lifshitz normal form [22],

$$\partial_t u = \eta + \mu u - u^3 + \nu \partial_{xx} u - \partial_{xxxx} u + d u \partial_{xx} u + c (\partial_x u)^2, \quad (2)$$

where  $\partial_x \sim \mu^{1/4}$ ,  $\nu \sim \mu^{1/2}$  accounts for the intrinsic length of the system (diffusion),  $d \sim O(1)$  and  $c \sim O(1)$ . The term  $\partial_{xxxx} u$  describes a super-diffusion, accounting for the short distance repulsive interaction, whereas the terms proportional to  $d$  and  $c$  are, respectively, the non-linear diffusion and convection. The full and lengthy expressions of these coefficients, as a function of the LCLV parameters, will be reported elsewhere [31]. Note that

the same model has been recently deduced for instabilities in a semiconductor laser [21].

The model shows bistability between a homogeneous and a spatially periodic solutions and therefore exhibits a family of localized structures. Depending on the choice of parameters, localized structures may show periodic or aperiodic oscillations of their position. We can fix  $\mu$  and  $\eta$  by varying  $V_0$  and  $I_{in}$ . More interesting is the behavior of the effective diffusion term  $\nu$ , which has the form  $\nu \propto l^2 + (\pi\beta L \cos^2(\beta/2 \cos^2 \theta_o) \sin 2\theta_o)/4k((TV_o + \alpha I_{in}(1 + \cos(\beta \cos^2 \theta_o)))$ . Only when the optical free propagation length  $L$  is negative it is possible, by increasing the input intensity  $I_{in}$ , to drive the system through the Lifshitz point ( $\nu$  changes its sign from positive to negative). This means that stable localized structures can be obtained only for a focusing Kerr-like nonlinearity. Once crossed the Lifshitz point, the nonlinear diffusion coefficient is negative and the convection coefficient is positive. In this region of parameters, numerical simulations of Eq.(2) show a qualitative agreement with the experimental observations, as shown in Fig.7.

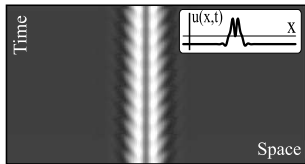


FIG. 7: Numerical simulations of Eq. (2) for  $\eta = -0.02$ ,  $\mu = -0.02$ ,  $\nu = -1.00$ ,  $c = 2.00$  and  $d = -1.51$ , showing two bouncing localized structures (spatial profile in the inset).

*Conclusions.* We have shown a new kind of localized structure dynamics, consisting of a bouncing behavior between two adjacent structures, and we have described it by an universal model, the Lifshitz normal form equation. The Lifshitz equation, that reduces to the generalized Swift-Hohenberg equation for  $\eta = d = c = 0$ , has already been used to describe the transition from smectic to helicoidal phase in liquid crystals [32] and the pulse dynamics in reaction diffusion systems [33]. When one neglects the cubic and the nonlinear diffusion terms ( $d = 0$ ), it reduces to the Nikolaevskii equation that describes longitudinal seismic waves [34].

We gratefully acknowledge René Rojas for help in calculations. The simulation software *DimX* is property of INLN. This work has been supported by the ACI Jeunes of the French Ministry of Research (2218 CDR2). M.G. Clerc thanks the support of Programa de inserción de científicos Chilenos of Fundación Andes, FONDECYT project 1020782, and FONDAP grant 11980002.

- [2] S. Pirkl, P. Ribiere and P. Oswald, *Liq. Cryst.* **13**, 413 (1993).
- [3] Y.A. Astrov and Y.A. Logvin, *Phys. Rev. Lett.* **79**, 2983 (1997).
- [4] K-Jin Lee, W. D. McCormick, J.E. Pearson and H.L. Swinney, *Nature* **369**, 215 (1994).
- [5] J. Wu, R. Keolian and I. Rudnick, *Phys. Rev. Lett.* **52**, 1421 (1984).
- [6] B. Denardo, W. Wright, S. Putterman and A. Larraza, *Phys. Rev. Lett.* **64**, 1518 (1990).
- [7] W.S. Edwards and S. Fauve, *J. Fluid Mech.* **278**, 123 (1994).
- [8] P.B. Umbanhowar, F. Melo and H.L. Swinney, *Nature* **382**, 793 (1996).
- [9] R. Heinrichs, G. Ahlers and D.S. Cannell, *Phys. Rev. A* **35**, R2761 (1987).
- [10] P. Kolodner, D. Bensimon and C.M. Surko, *Phys. Rev. Lett.* **60**, 1723 (1988).
- [11] D.W. Mc Laughlin, J.V. Moloney and A.C. Newell, *Phys. Rev. Lett.* **51**, 75 (1983).
- [12] R. Neubecker, G.L. Oppo, B. Thuring and T. Tschudi, *Phys. Rev. A* **52**, 791 (1995).
- [13] B. Schäpers, M. Feldmann, T. Ackemann and W. Lange, *Phys. Rev. Lett.* **85**, 748 (2000).
- [14] S. Barland *et al.*, *Nature* **419**, 699 (2002).
- [15] M. Cross and P. Hohenberg, *Rev. Mod. Phys.* **65**, 581 (1993).
- [16] P. Couillet, *Int. J. of Bif. & Chaos* **12**, 245 (2002).
- [17] S. Fauve and O. Thual, *Phys. Rev. Lett.* **64**, 282 (1990).
- [18] P. Couillet, C. Riera and C. Tresser, *Phys. Rev. Lett.* **84**, 3069 (2000).
- [19] see O. Descalzi, Y. Hayase and H.R. Brand, *Phys. Rev. E* **69**, 026121 (2004) and references therein.
- [20] M. Tlidi, P. Mandel, and R. Lefever, *Phys. Rev. Lett.* **73**, 640 (1994).
- [21] G. Kozyreff, S.J. Chapman and M. Tlidi, *Phys. Rev. E* **68**, 015201(R) (2002); G. Kozyreff and M. Tlidi, *Phys. Rev. E* **69**, 066202 (2004).
- [22] M.G. Clerc, to be published in *Phys. Lett. A* (2004).
- [23] P.L. Ramazza, S. Ducci, S. Boccaletti and F.T. Arecchi, *J. Opt. B* **2**, 399 (2000).
- [24] Y. Iino and P. Davis, *J. of Appl. Phys.* **87**, 8251 (2000).
- [25] P.L. Ramazza *et al.*, *Phys. Rev. E* **65**, 066204-1 (2002).
- [26] S. Residori, T. Nagaya and A. Petrossian, *Europhys. Lett.* **63**, 531 (2003).
- [27] Further details can be found on the web site of the manufacturer : <http://www.niopik.ru>
- [28] M.G. Clerc, S. Residori, C.S. Riera, *Phys. Rev. E* **63**, 060701(R), (2001).
- [29] M.G. Clerc, T. Nagaya, A. Petrossian, S. Residori and C.S. Riera, *Eur. Phys. J. D* **28**, 435 (2004).
- [30] R.M. Hornreich and M. Luban, *Phys. Rev. Lett.* **35**, 1678 (1975).
- [31] M.G. Clerc, R. Rojas, A. Petrossian and S. Residori, preprint 2004.
- [32] A. Michelson, *Phys. Rev. Lett.* **39**, 464 (1977).
- [33] R. Kobayashi, T. Ohta and Y. Hayase, *Phys. Rev. E* **50**, R3291 (1994).
- [34] M.I. Tribelsky and K. Tsuboi, *Phys. Rev. Lett.* **76**, 1631 (1996).

---

[1] H.A. Eschenfelder, *Magnetic Bubble Technology* (Springer Verlag, Berlin 1981).

